Biomacromolecules

ARTICLE

pubs.acs.org/Biomac

Protein Purification by Polyelectrolyte Coacervation: Influence of Protein Charge Anisotropy on Selectivity

Yisheng Xu,[†] Malek Mazzawi,[†] Kaimin Chen,[§] Lianhong Sun,[‡] and Paul L. Dubin*[,†]

[†]Department of Chemistry and [‡]Department of Chemical Engineering, University of Massachusetts, Amherst, Massachusetts, 01003

[§]State Key Laboratory of Chemical Engineering, School of Chemical Engineering, East China University of Science and Technology, Shanghai, 200237, P. R. China

ABSTRACT: The effect of polyelectrolyte binding affinity on selective coacervation of proteins with the cationic polyelectrolyte, poly(diallyldimethylammonium chloride) (PDADMAC), was investigated for bovine serum albumin/β-lactoglobulin (BSA/BLG) and for the isoforms BLG-A/BLG-B. High-sensitivity turbidimetric titrations were used to define conditions of complex formation and coacervation (pH_c and pH_ϕ, respectively) as a function of ionic strength. The resultant phase boundaries, essential for the choice of conditions for selective coacervation for the chosen protein pairs, are nonmonotonic with respect to ionic strength, for both pH_c and pH_ϕ. These results are explained in the context of short-range attraction/long-range repulsion governing initial protein binding "on the wrong side of pI" and also subsequent phase separation due to charge neutralization. The stronger binding of BLG despite its higher isoelectric point, inferred from lower pH_c, is shown to result from the negative "charge patch" on BLG, absent for BSA, as visualized via computer modeling (DelPhi). The higher affinity of BLG versus BSA was also confirmed by isothermal titration calorimetry (ITC). The relative values of pH_ϕ for the two proteins show complex salt dependence so that the choice of ionic strength determines the order of coacervation, whereas the choice of pH controls the yield of the target protein. Coacervation at I = 100 mM, pH 7, of BLG from a 1:1 (w/w) mixture with BSA was shown by SEC to provide 90% purity of BLG with a 20-fold increase in concentration. Ultrafiltration was shown to remove effectively the polymer from the target protein. The relationship between protein charge anisotropy and binding affinity and between binding affinity and selective coacervation, inferred from the results for BLG/BSA, was tested using the isoforms of BLG. Substitution of glycine in BLG-B by aspartate in BLG-A lowers pH_c by 0.2, as anticipated on the basis of DelPhi modeling. The stronger binding of BLG-A, confirmed by ITC, led to a difference in pH_ϕ that was sufficient to provide enrichment by a factor of 2 for BLG-A in the coacervate formed from "native BLG".

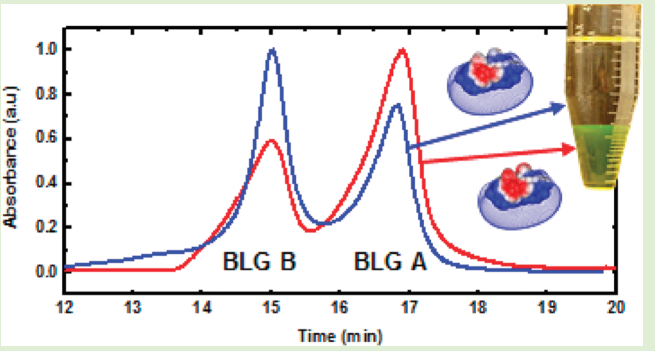

INTRODUCTION

A major driving force behind current efforts to develop a variety of efficient methods for protein purification[1−3] is the growing demand for recombinant proteins,[4−6] for example, monoclonal antibodies, cytokines, and subunit vaccines. As an example, the estimated value of recombinant protein factor VIII needed to satisfy the total market is on the order of ≈ $1 billion.[7] Despite this growing demand, downstream protein purification has lagged behind recombinant technologies and is usually an expensive and slow process. This high cost and slow speed creates a bottleneck in pharmaceutical process development that makes the need for efficient and high-yield protein separation technologies urgent.

Currently, commercial bioseparation techniques have not evolved far from familiar combinations of a relative limited variety of techniques, all of which have their virtues and drawbacks. For example, liquid chromatography and membrane separation are two major techniques that have been widely applied in industrial protein separations. The many forms of liquid chromatography offer high resolution and good selectivity but are limited by low throughput and large solvent consumption.[8] Membrane-selective permeation, offering higher throughput and greater economy, is developing as an alternative large-scale separation technique based on selectivity of the membrane stationary phase, for example, ion exchange, affinity, and hydrophobicity.[9] However, applications of selective membranes are limited to some extent by low binding capacity of analytes arising from low membrane surface area. The quality of membranes, for example, uniformity of pore size, stability of coatings, and evenness of thickness, also strongly influences the performance of separation.[9] Because of these limitations, there is a need for large scale, economic, and highly selective separation techniques as alternatives to liquid chromatography and membrane separation.

Received: December 4, 2010
Revised: February 9, 2011

Phase separation based on protein precipitation by salts,[10] organic solvents,[11] or polyelectrolytes[12−15] provides an alternative to the above-mentioned techniques for protein purification.[16] The important features of these separation techniques are: (1) large purification capacity, (2) solvent economy and low cost, (3) high speed, and (4) simplicity with respect to instrumentation. Among the several precipitation methods noted, polyelectrolyte−protein precipitation can offer selectivity, but recovery of proteins can be complicated with regard to preservation of protein activity[17,18] and redissolution.[19,20] In contrast, phase separation by polyelectrolyte coacervation is a "soft method" in which protein−polyelectrolyte complexation is fully reversible and protein stability can be retained,[21] as indicated by the lack of change in protein circular dichroism[22] or, more sensitively, by the absence of any reduction in enzyme activity.[23]

Complex coacervation is a liquid−liquid phase separation that occurs in solutions of oppositely charged macromolecules, including both polyelectrolytes and charged colloidal particles. Phase separation occurs subsequent to the formation of soluble complexes under critical conditions of ionic strength and colloid surface charge density.[24] For protein−polyelectrolyte systems, the colloid charge density is pH-dependent, and a critical pH for complexation known as "pH_c" marks the binding of multiple proteins to a single polymer chain.[25,26] This pH_c depends only on ionic strength and the protein of interest, not macromolecular concentrations or polymer molecular weight.[27] It appears likely that the formation of multipolymer soluble aggregates of these primary complexes is an intermediate stage.[28] Coacervation occurs when these soluble complexes or aggregates approach charge neutrality, that is, when the number and charge of the bound proteins compensate for the charge of the polyelectrolyte.[29] The corresponding condition "pH_ϕ" requires a protein net charge opposite to the polyelectrolyte, in contrast with pH_c, which may occur even when protein charge and polyelectrolyte are of the same sign.[30] The driving force for coacervation appears to be the replacement of protein- and polyelectrolyte-bound counterions by protein−polyelectrolyte interactions and the corresponding increase in entropy from counterion release.[31] This loss of counterions goes hand-in-hand with desolvation, leading to a dense viscous fluid that contains 70−80% water with protein concentrations of 15−25% (w/w).[32,33]

Selectivity in protein−polyelectrolyte coacervation might be considered a result of differences in pI at a given pH, a more acidic protein would bind to a polycation more readily than does a basic protein. However, proteins of nearly equal pI can show wide differences in pH_c, a result of charge anisotropy.[30] Furthermore, proteins with equal pH_c, a rough indication of similar binding constants, might form complexes that attain charge neutrality and hence coacervation at different pH. Consequently, it would seem difficult to predict the feasibility of selective coacervation and to optimize the conditions for attaining it. Charge anisotropy affects protein−polyelectrolyte binding, and coacervation is not ruled by simple consideration of pIs; but whether subtle differences in surface charges can lead to selective binding has not been systematically explored.

There has long been an assumption that protein separations based on nonspecific interactions lack the selectivity of methods like affinity chromatography and that the only way to introduce selective separation is via epitopes (protein recognition sites) governed by short-range, specific interactions.[34,35] However, the ability of ion exchange chromatography (IEC)[36] to separate proteins with small charge differences provides an example of high selectivity based on electrostatics.[37,38] The fact that both ion-exchange resins[39] and polyelectrolyes[25,40,41] can bind protein "on the wrong side of pI" means they are both responsive to protein domains of opposite charge. If polyelectrolyte binding is sensitive to small differences in protein charge domains ("charge patches"), then highly selective complexation can occur under appropriate pH conditions, as it does in IEC. Because coacervation arises from soluble protein−polyelectrolyte complexes, selective complexation might be correlated with selective coacervation, meaning that macroscopic phase separation arises from microscopic short-range electrostatic interactions. In this way, detailed consideration of protein charge distribution could become a predictive tool that circumvents the trial-and-error approach characteristic of many large scale protein purification schemes.

Optimization of selective coacervation requires identification of conditions of pH and ionic strength at which only the target protein forms coacervate. For polycations, for example, pH must be above pH_ϕ for the target protein but below pH_ϕ for "contaminant" protein(s). However, pH_ϕ, corresponding to phase separation and charge neutrality reflects in complicated ways net protein charges and stoichiometries.[27] A better measure of protein−polyelectrolyte binding affinity is pH_c, which corresponds to the condition of incipient binding, at which binding energy proportional to log K_{obs} (K_{obs} is binding constant) is close to thermal energy (kT). Whereas the exact relationship between $\Delta pH = |pH - pH_c|$ and logK_{obs} is not known, this indirect measure of binding energy makes it possible to qualitatively correlate affinity to protein structure. The ionic strength dependence of pH_ϕ and pH_c are therefore "phase boundaries", which both provide practical guidelines[21] and help relate differences in binding affinities to selective phase behavior.[42]

Our purpose here is to examine the relationship between protein charge patch density and pH_c and establish how the corresponding binding affinity can control coacervation at pH_ϕ. We use binding to a strong polycation poly(diallyldimethylammonium-chloride) (PDADMAC) in combination with two proteins bovine serum albumin (BSA) (pI ∼4.9) and β-lactoglobulin (BLG) (pI ∼5.2), which resemble each other only with respect to pI, and two protein isoforms that differ only with respect to two amino acids. We find that the lower value of pH_c for BLG as compared with that of BSA is correlated with its larger binding constant, as measured by isothermal titration calorimetry (ITC). The relative values of pH_ϕ for the two proteins show complex salt dependence so that the choice of ionic strength determines the order of coacervation.[43] Further enhancement of the BLG negative domain is provided by BLG-A, a genetic variant in which a neutral residue in the charge patch of the BLG-B monomer is replaced by a negative one. The subtle charge difference between the two variants resulted in significant differences in both pH_c and pH_ϕ, demonstrating that apparently subtle differences in nonspecific electrostatic interactions lead to selective coacervation.

EXPERIMENTAL SECTION

Materials. The PDADMAC sample (gift from W. Jaeger, Fraunhofer, Golm) was prepared by free radical aqueous polymerization of diallydimethylammonium chloride[44] and characterized after dialysis and lyophilization by membrane osmometry (M_n = 141 kDa) and light scattering (M_w = 219 kDa). Bovine serum albumin (68 kDa) with total free acid content ≤1.2 mg/g was purchased from Roche Diagnostics

(Indianapolis, IN; CAS 9048-46-8). BLG (18 kDa, referred to below as "native BLG") was a gift from C. Schmitt (Nestle, Lausanne). We established by ion-exchange chromatography (see below) that this sample consisted (at neutral pH) of AA and BB dimers only. Isoforms of BLG (BLG-A and BLG-B) were obtained as lyophilized powders (batch Nos. 2010001 and 06101001, respectively) from NIZO (Wageningen, Netherlands). NaCl, sodium acetate, sodium phosphate (monobasic), and standard NaOH, HCl, and acetic acid solutions were purchased from Fisher Scientific. Milli-Q water was used in all sample preparation.

Turbidimetric Titrations. PDADMAC solutions (0.24 g/L) and protein (BSA, BLG, BLG-A, and BLG-B) solutions (1.2 g/L) were prepared separately at the desired concentration of NaCl (5−200 mM) and at pH 3 to 3.5, and filtered (0.22 μm Millipore). We mixed 5 mL of each solution to a final volume of 10 mL. Turbidimetric titration was carried out by the addition of 0.01 N NaOH to a total solution volume of 10.0 mL in increments of ∼0.1 pH unit, up to a final pH of 10, with stirring and simultaneous monitoring of pH and transmittance. Transmittance was measured using a Brinkmann PC 800 colorimeter equipped with a 2 cm path length fiber optics probe and a 450 nm filter, and pH was measured with a Corning 240 pH meter. The titration was completed in <15 min to minimize effects of protein aggregation. After suitable warm-up, the instrument drift over this time period was verified as <0.05% (in %T).

Preparation of Mixed Coacervates. To observe separation of BSA and BLG by coacervation, we first codissoloved BSA, BLG, and PDADMAC for 2 h in pH 3.5, I = 100 mM (NaCl) Milli-Q water to give a solution 12 g/L in BSA, 12 g/L in BLG, and 2.4 g/L in PDADMAC. pH was adjusted to 7 by the addition of 1 N NaOH, to form the mixed coacervate. To observe the separation of BLG-A from BLG-B, native BLG and PDADMAC were codissolved at 6 and 0.6 g/L, respectively, at pH 3.5, I = 100 mM NaCl. The solution was adjusted from pH 3.5 to 6.3, to form the mixed coacervate. For both the BSA/BLG system and the native BLG system, the turbid coacervates as described above were centrifuged (Beckman Coulter Allegra 6R) 1 h at 3700 rpm, 20 °C to produce an optically clear dilute (upper) and dense (lower) phase (coacervate). Coacervate was slowly removed by using a long needle syringe.

Size Exclusion Chromatography. To quantitate protein and polymer in (1) coacervate, (2) supernatant, (3) retentate after ultrafiltration, and (4) in concentrated filtrate after ultrafiltration in (BSA/BLG system), we carried out SEC on a prepacked Superose 6 HR 10/30 column using a Shimadzu Prominence LC system equipped with a refractive index detector (RID-10A), with 20 μL injections. The mobile phase was 150 mM NaCl + 30 mM acetate buffer (pH 4) at 0.40 mL/min. Initial solutions were directly analyzed after filtration. For the analysis of coacervate, 0.1 mL was dissolved with 0.4 mL of water (pH 3.5) and analyzed by SEC. After ultrafiltration, the retentate and concentrated filtrate were directly analyzed by SEC.

Isothermal Titration Calorimetry. ITC was carried out using a model VP-ITC (Microcal, Northampton, MA). For BSA/PDADMAC or BLG/PDADMAC, proteins and PE solutions were made in pH 5.3 buffer containing 10 mM phosphate and 90 mM NaCl. For BLG-A/PDADMAC and BLG-B/PDADMAC, proteins and PE were dissolved in pH 7 buffer containing 10 mM phosphate and 140 mM NaCl. All solutions were filtered (0.22 μm Millipore). After instrument stabilization for at least 1 h at 25 °C, 1.445 mL of 1 g/L (6.2 mM basis monomer repeat unit) PDADMAC solution was titrated with 40 successive injections of protein solutions (1 mM for BSA/BLG system and 1.2 mM for BLG-A and -B systems). The interval between injections was 400 s. The solution was stirred at 315 rpm in the reaction cell during the experiments. Prior to data analysis, heats of dilutions were corrected by subtracting values for polymer-free blank solutions. ITC data analysis typically employs canned software (e.g., Microcal Origin) which (1) converts raw calorimetric data (heat evolved or consumed for each titration step, $\delta\Delta H°$) to a binding isotherm, and (2) analyzes the binding isotherm to yield binding site number (size), and binding constant(s) from which $\Delta G°$ and hence $\Delta S°$ are obtained. The first step (1) is based on the assumption that any decrease in $\delta\Delta H°$ relative to its initial value is due to incomplete binding of the titrant molecules, this fundamental paradigm following the model of protein−ligand interactions. In our system, thermograms were transformed into binding isotherms by the methods described by Tomme[45] and Girard.[46] The second step (2) is model-dependent, that is, based on a model of a protein binding a single ligand to one or two binding sites, and thus applied to binding isotherms that show either a single or two inflection points. This model is inapplicable to protein−polyelectrolyte systems. The Scatchard plot used to fit the isotherm in ref 45 is less appropriate when the protein is the ligand, which is the case here as in ref 46. Therefore, the McGhee−Von Hippel model was used to fit the binding isotherms.[47]

Anion Exchange Chromatography. Anion exchange chromatography (Biorad UNO Q-1) was used to analyze the BLG-A/-B composition of native BLG before and after coacervation. We loaded 50 μL of protein sample (initial native BLG and supernatant) in the column equilibrated with pH 7, 20 mM Tris buffer and eluted at 1 mL/min with UV detection at 280 nm. A linear gradient was applied from 0 to 0.3 M NaCl from 2 to 32 min. Analysis of coacervate was preceded by SEC of acidified coacervate to remove PDADMAC; 50 μL of the SEC BLG fraction was then directly analyzed.

Computational Methods. Computer modeling was used to visualize the electrostatic potential around the protein as a function of pH and ionic strength. DelPhi V98.0 (Molecular Simulations) was used to calculate electrostatic potential around the protein is calculated by nonlinear solution of the Poisson - Boltzmann equation.[48] The protein crystal structures with Protein Data Bank identifications 1AO6 (HSA), 1BEB (BLG dimer) were taken from the RCSB Protein Data Bank (http://www.rcsb.org). Because the structure of 1BEB is the combination of BLG-A and -B, the electrostatic calculations were modified by replacing Gly64 with Asp64 to mimic a BLG-A dimer, and by replacing Val 118 with Ala118 to mimic a BLG-B dimer. The charges of amino acids were generated using the spherical-smeared-charged model proposed by Tanford[49] utilizing the protein titration curve of proteins,[50,51] as described elsewhere.[52]

Removal of PDADMAC by Ultrafiltration. In the BSA/BLG system, 50 μL of coacervate made as above was redissolved in 0.55 mL of water (pH ∼3.5) to reverse PE−protein complexation (this solution was analyzed by SEC to calculate the composition of coacervate); then, the redissolved coacervate was diluted to 20 mL with water at pH 3.5. Ultrafiltration was performed under 10 psi pressure using a polyethersulfone (Amicon) membrane with nominal molecular weight limit (NMWL) of 100 kDa. After ultrafiltration, 0.3 mL of retentate (rich of PDADMAC) was obtained, and the 20 mL filtrate was concentrated by freezing under vacuum overnight.

RESULTS AND DISCUSSION

1. BSA and BLG. Turbidimetric titrations were performed by the addition of NaOH to an acidic solution of protein and PDADMAC to determine the transition, first to soluble complex formation (pH_c) and then to phase separation (pH_ϕ). The results are shown in Figures 2 and 3. It is necessary to point out that the determination of pH_c can be complicated by protein aggregation, as shown by the initial nonzero slope in Figure 1. Optimally, a zero slope at low pH indicates the absence of complexation, but here this nonzero slope is due to BSA aggregation. Reduction of the titration time to 10−15 min effectively eliminated this behavior at the ionic strengths studied.

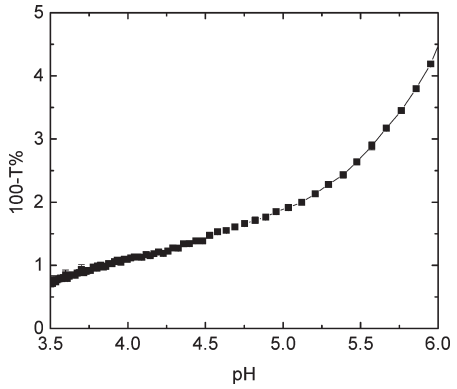

Figure 1. Turbidimetric titration of BSA-PDADMAC with addition of NaOH. [BSA] = 0.6 g/L, [PDADMAC] = 0.12 g/L, I = 30 mM. Time interval between pH 3.5 and 6 is ca. 60 min.

The parallel appearance of the "type 1 titrations" at all ionic strengths (Figure 2) strengthens identification of pH_c even in the presence of a nonzero slope, for example, at I = 0.02 M in Figure 2A. In contrast with the analysis of pH_c, the determination of pH_ϕ from Figure 3 is straightforward without expansion of any region. Some striking features of Figure 3 are the nonmonotonic salt effect and the presence of maxima under some conditions.

The nonmonotonic ionic strength dependence of both pH_c and pH_ϕ is most effectively shown by the phase boundaries obtained in Figure 4, as pH_ϕ and pH_c versus $I^{1/2}$. The well-defined pH_ϕ minima for BSA and BLG are clearly displaced with respect to each other and consequently cross at 50 mM. This is important for selective coacervation because BSA would preferentially be removed (by progressive increase in pH) at low salt and BLG at high salt. To understand this effect, we need to consider the origin of these minima and their relationship to the shallow minima of pH_c.

Identification of the minima of pH_c (~50 mM for both BLG and BSA), supported by the result for BSA/PDADMAC at ~30 mM already reported,[42] is made possible by the reliability of the data points: ± 0.2 (corresponding to symbol size) which is small compared with curvature. Seyrek[30] reported this behavior for several protein−polyanion systems that showed binding at pH > pI ("on the wrong side of pI"), indicating binding to a positive domain in the globally negative protein. The repulsive interaction with the negative domains must be long-range relative to the attractive interaction with the "positive patch". Maximum binding should occur when long-range repulsions are screened by small ions while short-range attraction is not. This should occur when the screening length (the "Debye length" ≈ $0.3I^{-1/2}$, in nanometers) is on the order of the protein radius, and this was consistent with $10 < I_{max} < 40$ mM.[30] In the present case, "binding on the wrong side of pI" corresponds to binding at pH < pI, with the significance of protein charge anisotropy vanishing at high pH where the globally negative protein binds to polycation.

The ionic strength dependences of pH_c and pH_ϕ are connected by the relationship between binding affinity and the number of proteins bound per polymer chain n_{pr}. At the point of coacervation, we have near neutrality for complex net charge[42]

$$Z_T = Z_P + n_{pr}Z_{Pr} \quad (1)$$

where Z_P is the charge of the polyelectrolyte (constant), and Z_{pr} is the charge of each protein (dependent on pH). While n_{pr} increases with binding affinity, we recognize that pH_c is an indirect, qualitative measure of the binding affinity at any pH. Although pH_c is presented as a phase boundary in Figure 4, this line does not correspond to a true phase transition. The appearance of a pH_c in Figure 2 means that the binding constant K_{obs} is negligibly small at pH < pH_c but then increases rapidly, with a corresponding increase in the number of bound proteins. At pH_c, the empirical onset of binding, the binding energy is close to kT. Thus, at a fixed pH (e.g., pH 5), n_{pr} and K_{obs} for BSA are largest at I_{max} = 50 mM where pH−pH_c shows a maximum.

While the curves for pH_c and pH_ϕ for BSA both show minima, these minima are clearly displaced with respect to each other. The minimum in pH_c arises from protein charge anisotropy, as described above, but the corresponding negative charge patch which is evident at pH < pI, disappears at high pH. Therefore, the nonmonotonic behavior of pH_ϕ, arising from an increase in protein−PE affinity with added salt in the low I range, must come from an effect other than the repulsion between the polycation and global protein charge. In the case of pH_ϕ, its increase with decreasing I, for I < 20 mM, now comes from a drop in n_{pr} due to repulsion between nearby bound proteins at pH > 6. In the range of 5 < I < 20 mM, the addition of salt screens these interprotein forces, increasing n_{pr} and thereby providing charge neutrality at low pH (less negative Z_{pr}). At higher I, the short-range PE−-protein interaction is screened, so that n_{pr} decreases for a different reason, so requiring more negative Z_{pr}, that is, higher pH. Therefore, even though minima in pH_c and pH_ϕ are both observed at I = 20−50 mM and both correspond to local maxima in n_{pr}, the drops with added salt for pH_c and pH_ϕ at low I arise from different causes. In the case of pH_ϕ, the low I region indicates that a small increase in ionic strength must be compensated by a large decrease in pH. In the high I region, a small increase in pH compensates for a large increase in salt. For the first case, pH controls interprotein repulsion through net protein charge; in the second case, pH controls binding through protein charges at the polyelectrolyte binding site. Because the polycation binding site on the protein by definition will be enriched in acidic residues, an increase in their degree of ionization results in a significant change in local potential, whereas the same effect on global charge only modestly increases interprotein repulsion. Put differently, the Debye length, proportional to $I^{-1/2}$, changes strongly with I at low salt but more slowly at high salt.

BLG preferentially coacervates at I > 50 mM, the same region where the pH_c curves of the two proteins diverge: the addition of salt diminishes the affinity of PDADMAC for BSA more than its affinity for BLG. The persistence of low pH_c (high polycation affinity) for BLG is a consequence of the retention of its negative charge patch at higher I. The DelPhi images in Figure 5 show that the small negative domains (red) for BSA at I = 5 mM shrink and become almost invisible to PDADMAC when the ionic strength is raised to I = 150 mM. However, the negative patch of BLG is largely kept intact even though the positive charge patch shrinks significantly under high salt condition. Put differently, the polycation-binding domains for BSA are more diffuse than those for BLG and therefore require a globally negative net protein charge (higher pH) at higher I. The retention of stronger binding for BLG with increasing I appears to explain why BLG coacervates preferentially.

The shift in preferential coacervation from BSA to BLG with increasing I is manifested in the crossing of the pH_ϕ curves at I = 50 mM, pH 6.3. This crossover point in Figure 4 corresponds to the pH, I condition at which the coacervation preference changes

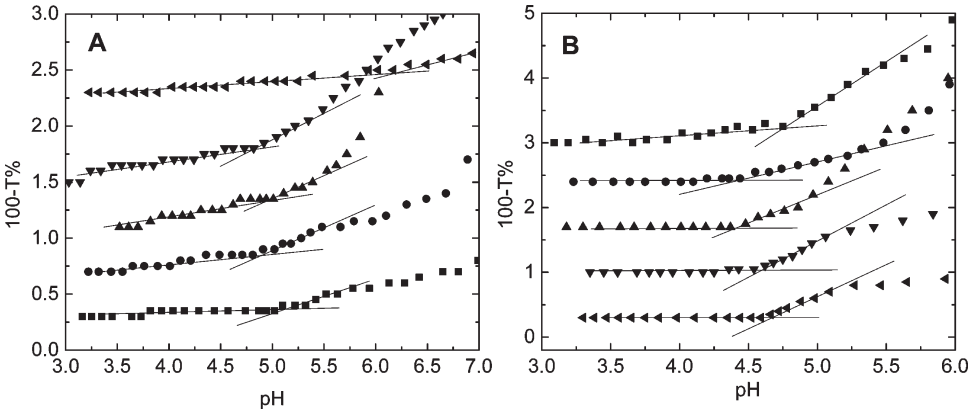

Figure 2. Determination of transition for BSA/BLG-PDADMAC at various ionic strengths corresponding to soluble complex formation (pH_c). (A) [BSA] = 0.6 g/L, (B) [BLG] = 0.6 g/L, [PDADMAC] = 0.12 g/L. For BSA, from bottom to top: 5, 10, 20, 100, and 200 mM. For BLG, from bottom to top: 5, 10, 30, 100, and 200 mM.

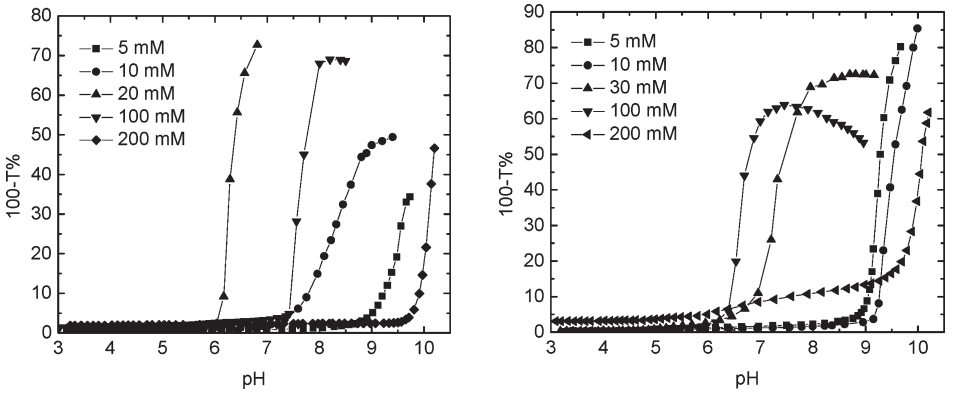

Figure 3. Turbidimetric titrations for BSA (left) and BLG (right) at different ionic strengths, protein, and polymer concentration are 0.6 and 0.12 mg/mL, respectively.

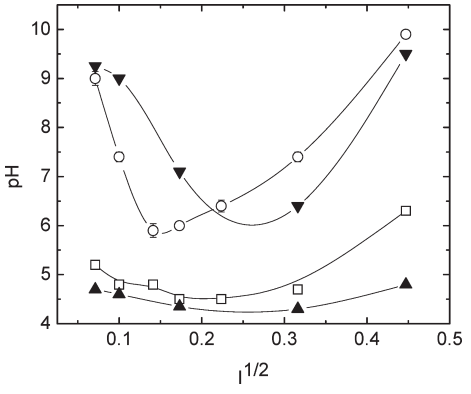

Figure 4. Phase boundary of BSA and BLG with PDADMAC from data of Figures 2 and 3. pH_c: BSA (□), BLG (▲); pH_ϕ: BSA (○), BLG (▼).

from BSA to BLG; this happens at pH 6.3. To understand this, we plotted the ratio of the charges of the two proteins in Figure 6 and found that this is the pH at which the net (negative) charge of BSA begins to exceed the net negative charge of BLG. Under this condition, selective coacervation is impossible. From eq 1 and the electroneutrality assumption, this condition corresponds to $Z_{pr}^{BSA}/Z_{pr}^{BLG} = n_{BLG}/n_{BSA}$. The crossover point must arise because a decrease in n_{BSA}/n_{BLG} compensates for an increase in $Z_{pr}^{BSA}/Z_{pr}^{BLG}$. We obtained the latter ratio from data of Tanford[50,51] and plot it as a function of pH in Figure 6; at the crossover point, $Z_{pr}^{BSA}/Z_{pr}^{BLG} = 1.2$, so that n_{BLG}/n_{BSA} must be 1.2. This slightly preferential binding for BLG is consistent with its slightly lower pH_c at $I = 50$ mM. At this ionic strength, we may imagine an increase in pH allowing entrance into the coacervation region at pH 6.3 for both proteins because the higher charge of BSA compensates for its slightly lower affinity. Imagining an increase in ionic strength at pH 6.3, the coacervation region for BLG is entered at $I = 50$ mM simultaneous with exiting from the coacervation region for BSA. $I = 50$ mM might be the condition at which the greater salt-resistance of the affinity of BLG, seen from the divergence of the pH_c curves, begins to overcompensate for its lower charge.

We have discussed the features of the phase boundaries of BSA and BLG because it is the difference between the respective coacervation points ($\Delta pH_\phi = pH_\phi^{BSA} - pH_\phi^{BLG}$) that makes separation possible.[43] As noted above, ΔpH_ϕ appears to be correlated with ΔpH_c ($pH_c^{BSA} - pH_c^{BLG}$); this is because pH_c reflects the binding affinity of protein to polyelectrolyte. Because ΔpH_c is not a meaningful thermodynamic quantity, we did ITC to measure the difference in polycation binding constants for the two proteins (ΔK_{obs}). For ITC conditions, we chose $I = 100$ mM because, as shown in Figure 4, ΔpH_c is large, and ΔpH_ϕ is

dx.doi.org/10.1021/bm101465y |*Biomacromolecules* XXXX, XXX, 000–000

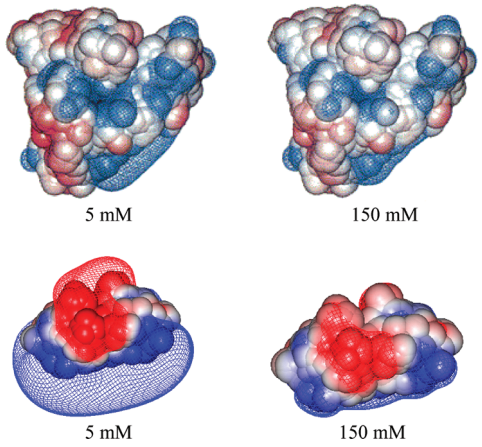

Figure 5. Electrostatic potential contours (−0.5 (red) and +0.5 (blue) kT/e) around the BSA (upper, from ref 40) at pH 5.6 and BLG dimer (lower, from ref 56) at pH 5.

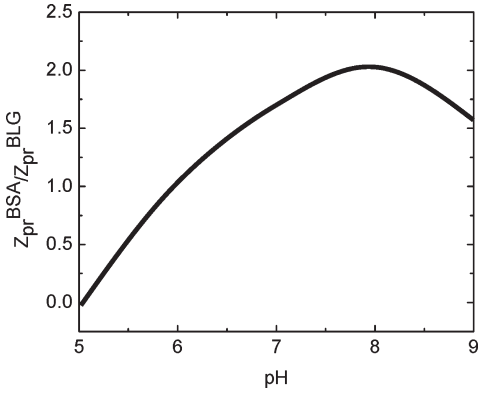

Figure 6. pH-dependent net charge of BSA (monomer) divided by the net charge of BLG dimer obtained from refs 50 and 51.

positive and close to its maximal value. We chose pH 5.3 to ensure that the system is in the soluble complex region and also because its proximity to pI will ensure the influence of charge anisotropy.

Figure 7 shows raw ITC data for PDADMAC with BSA and with BLG. The vertical peaks correspond to the heat change in the cell containing PDADMAC at each protein injection. For BSA, the peaks gradually convert from downward to upward because the complexation between BSA and PDADMAC is exothermic whereas the dilution of BSA is endothermic (blank BSA dilution experiment not shown). Whereas the measurement of the heat of binding by ITC is straightforward, the values of entropy or energy obtained are model-dependent. For the BLG−pectin system, Girard and coworkers[46] analyzed the binding isotherms using the overlapping binding site (McGhee−von Hippel) model. This model describes the binding of interacting (cooperative) or noninteracting ligands to a homogeneous 1D lattice (host), which seems more appropriate to the present case, in which one polyelectrolyte can bind many proteins, than do models in which the protein is the host. The fitting parameters are n, K_{obs}, and ligand−ligand cooperativity.[47] For noninteracting ligands, the binding model takes on a form analogous to the Scatchard formulation[52,53]

$$\frac{\nu}{L} = K_{obs}(1 - n\nu)\left(\frac{1 - n\nu}{1 - (n-1)\nu}\right)^{n-1} \quad (2)$$

In eq 2, ν represents the binding density expressing the number of ligands (proteins) bound per polymer repeat unit, closely related to the number bound per polymer chain (previously denoted as n_{pr}). L is the free-ligand concentration and n is the number of polymer units per bound protein molecule. n identifies the size of the binding site and is related to N_b, the number of binding sites per polymer molecule, by $N_b = x/n$, where x is the degree of polymerization. $N_b = n_{pr}$ under saturation binding conditions. The application of eq 2 to the BLG−pectin system in ref 46 led to a much higher number of binding sites (N_b) and consequently lower binding constants than those obtained with the "two-site" binding model. We proceeded to fit the raw data in Figure 7 to the McGhee−von Hippel binding model to obtain the intrinsic binding constant (K_{obs}), the binding site size (n), and the number of polymer repeat units per bound protein molecule.

All thermograms directly measured from ITC were transformed to obtain the binding density "ν" and free protein concentration "L" values following the method of Girard et al. for the binding of BLG to pectin.[46] The least-squares nonlinear curve fitting of ν plotted against L is shown in Figure 8 and the resultant K_{obs}, and n values in Table 1. The binding constant for BLG is between two and three times greater than the value for BSA, which confirms the qualitative observation from pH_c. As suggested from Figure 5, we propose that BLG binds more strongly to PDADMAC because of its concentrated negative charge patch. Therefore, the ITC results establish the connection between ΔpH_c and $\Delta(\Delta G)$.

The binding site sizes for BLG and BSA are n = 50 and 80, respectively. Expressed as contour lengths (based on the polymer repeat unit length of ca. 0.6 nm), these are 30 and 48 nm, respectively, both five to six times larger than the respective protein diameters of 5.5 and 8.0 nm. These contour length values (expressed as n) are similar to n = 22 reported for BLG−pectin[46] because the length of the pectin repeat unit is twice that of PDADMAC. The large protein-binding site size could arise from the repulsive interactions between charged neighboring proteins (anticooperative binding).

Whereas both the turbidimetric titration and microcalorimetry show stronger binding by BLG, the extent of separation possible is not evident from these results. From the titration of BLG + PDADMAC at I = 100 mM from pH 3−9 and in the presence and absence of BSA (Figure 9), it may be seen that BSA has no influence on the coacervation of BLG with PDADMAC. This indicates that proteins can interact independently with PDADMAC. After centrifugation of the BSA/BLG/PDADMAC mixture at pH 7 and I = 100 mM, three layers (from bottom to top) were identified as precipitate, coacervate, and supernatant. After acidification to pH 3.5 to effect redissolution, the coacervate was diluted and analyzed by SEC. The result for the coacervate is compared with those for supernatant and initial solution in Figure 10. (Data for the precipitate, which accounted for <10%, are not shown.) 90% of the protein in the coacervate is BLG, whereas BSA accounts for 85% of the protein in the supernatant. These results demonstrate a selective removal of BSA from the target protein BLG and a 20-fold increase in target protein concentration relative to the initial mixture.

dx.doi.org/10.1021/bm101465y |*Biomacromolecules* XXXX, XXX, 000–000

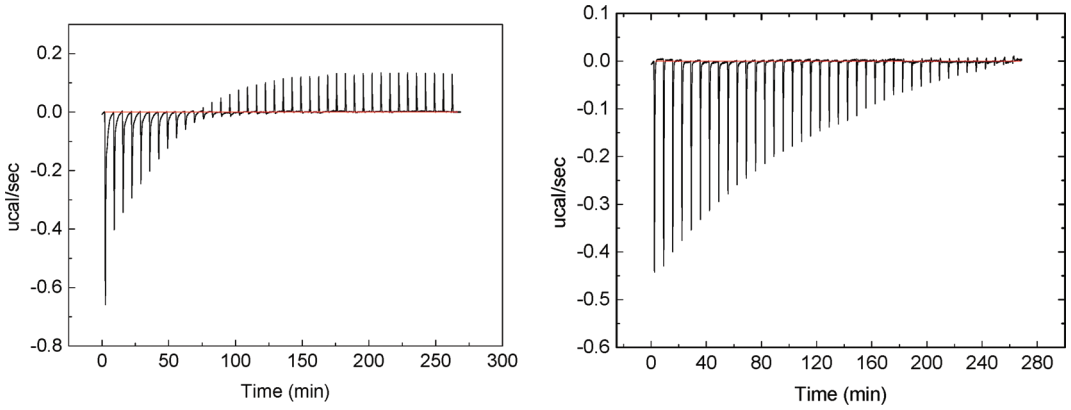

Figure 7. Isothermal calorimetry titration raw data for BSA-PDADMAC (left) and BLG-PDADMAC (right). Protein titrant, concentration 1 mM (18.7 g/L for BLG, and 66.8 g/L for BSA), was added to 6.2 mM (basis monomer repeat unit) (1 g/L) PDADMAC. Solvent (for both protein and polymer) 10 mM, pH 5.3 phosphate + 90 mM NaCl. incremental volume of titrant: 6 μL; injection in 14.4 s. Binding goes from exothermic to endothermic for BSA.

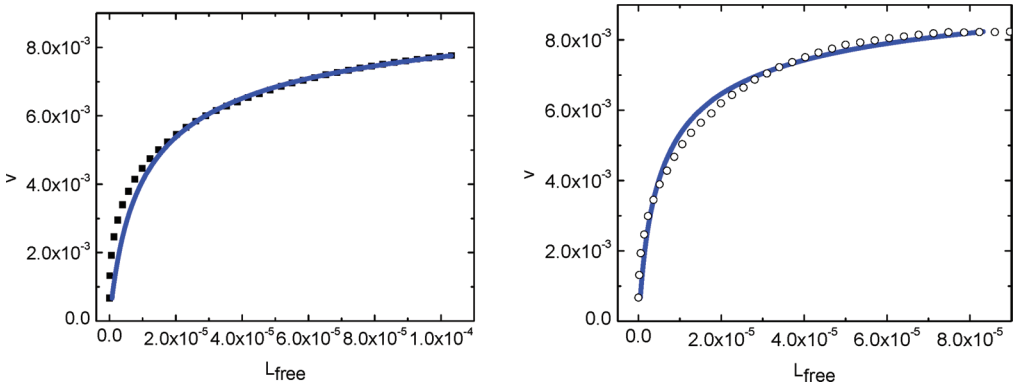

Figure 8. Binding isotherms of BSA-PDADMAC (left) and BLG-PDADMAC (right) transformed from Figure 7. Dotted lines are experimental binding isotherms; solid lines are nonlinear least-squares fitting to eq 2.

Table 1. Binding Parameters of BSA/BLG-PDADMAC at pH 5.3, I = 100 mM[a]

	K_{obs} (M^{-1})	n	ΔG (kcal/mol)
BSA	740 ± 30	80 ± 1.9	−3.89 ± 0.02
BLG	1900 ± 340	50 ± 1.1	−4.45 ± 0.11

[a] ΔG was calculated from binding constant.

2. BLG-A and BLG-B. In the previous section, we showed that the selective coacervation of BLG relative to BSA previously observed at high pH and ionic strength could be understood in terms of the phase boundaries in Figure 4. This was based on a correlation between conditions for the formation of soluble complexes and conditions for coacervation involving two factors: protein affinity, and protein (that is, n_{pr} and Z_{pr} in eq 1), with higher affinity for BLG due to its negative "charge patch". To validate the influence of such charge anisotropy while minimizing hypothetical differences between proteins arising from hydrophobicity and hydrogen bonding and without the need for site mutation, we turned to the BLG genetic variants A and B, in which the replacement of glycine by aspartate at position 64 appears to lead to a significant change in the negative charge patch of the BLG-A dimer with two additional aspartates

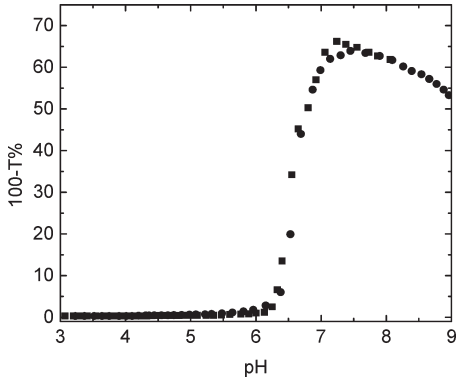

Figure 9. Turbidmetric titration of PDADMAC and BLG, with (■) and without (●) BSA. [BLG] = 0.6 g/L, [BSA] = 0.6 g/L, [PDADMAC] = 0.12 g/L, I = 100 mM NaCl.

(Figure 11). Whereas there have been a number of hypotheses about structural differences between these two variants,[54,55] the greatly increased electrostatically induced native state aggregation of the A form[56] is consistent with this enhanced negative charge domain. Here we choose to portray in Figure 11 the potential contour at 0.5 kT/e (13.5 mV) based on the proposals

dx.doi.org/10.1021/bm101465y |*Biomacromolecules* XXXX, XXX, 000–000

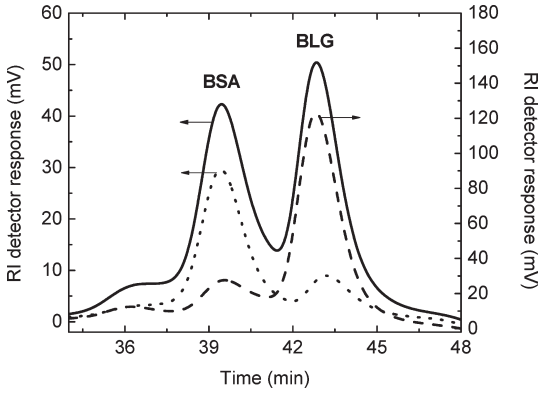

Figure 10. SEC analysis of composition of BSA and BLG in different phases. (a) Control (prior to coacervation): solid line, axis left. (b) Supernatant: dotted line, axis left. (c) Coacervate: dashed line, axis right. Only an early eluting broad peak for PDADMAC appears at low elution time (not shown).

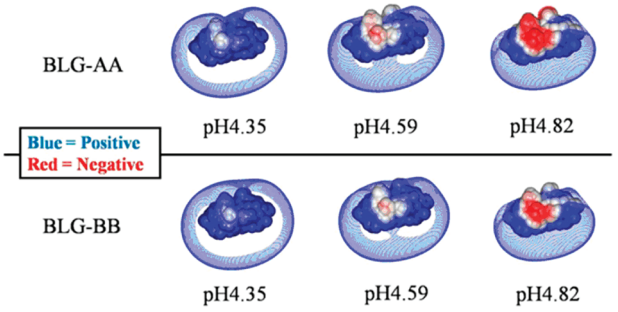

Figure 11. Electrostatic potential contours (−0.5 (red) and +0.5 kT/e (blue)) for dimers of BLG-A (above) and BLG-B (below) in 100 mM salt at pH values shown.[57]

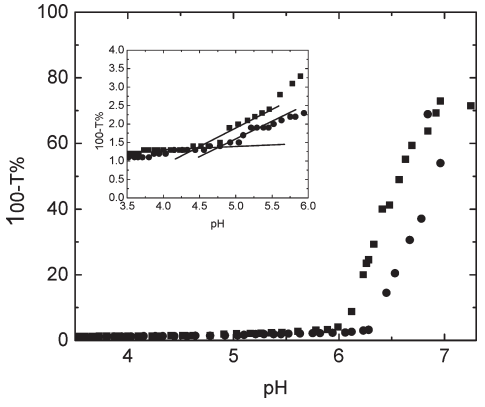

Figure 12. Turbidimetric titrations of BLG-A (■) and BLG-B (●) with PDADMAC in 100 mM NaCl. Protein concentration is 0.6 g/L and r = 5. Inset: pH_c determination for both proteins.

that (1) the interaction energy at pH_c (the onset of binding) should be close to kT and (2) the number of PDADMAC repeat (charge) units in this potential domain could be on the order of two (1.2 nm contour length); that is, two polyelectrolyte repeat units bound at the 0.5 kT/e region involve an interaction close to thermal energy. Enhancement of binding affinity and

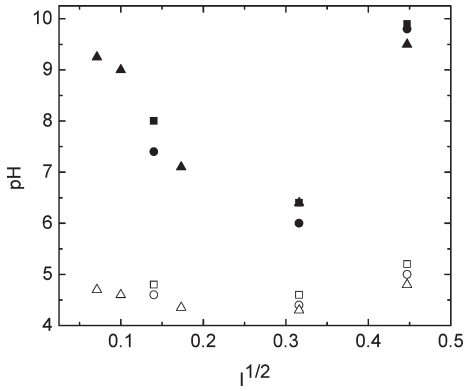

Figure 13. Phase boundary of BLG-A and -B. Protein and polymer concentrations are 0.6 and 0.12 g/L, respectively. pH_c: native BLG (△), BLG-A (○), BLG-B (□); pH_ϕ: native BLG (▲), BLG-A (●), BLG-B (■).

coacervation from this subtle difference in charge anisotropy between BLG-A and -B would suggest the general feasibility for selective coacervation based on electrostatics.

Following the same procedures those as for Figures 2 and 3, we obtained pH_c and pH_ϕ, as shown for example for 100 mM salt in Figure 12. The results for BLG-A and BLG-B at this ionic strength are: pH_c (4.4, 4.6); pH_ϕ (6.0, 6.3) with standard deviations from multiple runs of ±0.05 pH units. Because Z_p is nearly identical for the two variants, eq 1 then shows that the lower pH_ϕ for BLG-A comes only from $n_{pr}^{A} > n_{pr}^{B}$, that is, from $K_{obs}^{BLGA} > K_{obs}^{BLGB}$. This difference in affinity is also seen from $pH_c^{B} > pH_c^{A}$, so that the relationship between $\Delta pH_c = pH_c^{B} - pH_c^{A}$, on one hand, and $\Delta pH_\phi = pH_\phi^{B} - pH_\phi^{A}$,on the other hand, is simplified, relative to the BSA/BLG system.

The expectation of a relationship between ΔpH_ϕ and ΔpH_c for BLG-A versus BLG-B, more simple than the similar relationship found for BLG versus BSA, is borne out by Figure 13 in which values for all ionic strengths are presented. Here pH_ϕ for BLG-A is always lower than that for BLG-B, with the same pattern appearing more subtly for pH_c (although we cannot ignore the fact that pH_ϕ and pH_c values at each I come from the same plot and might share a common bias). No crossover point is observed, as was seen for BSA versus BLG in Figure 4. The explanation for that crossover point involved the difference in net charge of these two proteins ($Z_{pr}^{BSA}/Z_{pr}^{BLG}$) at most pH values. In the absence of any comparable effect from $Z_{pr}^{BLGA}/Z_{pr}^{BLGB}$, both ΔpH_ϕ and ΔpH_c arise from the difference in the charge patch. The influence of the two relevant aspartate residues disappears when the protein becomes highly negative, so the pH_ϕ curves for BLG-A and -B converge at pH >8.

Data for "native BLG" from Figure 4 are also included in Figure 13. Native BLG is a 52:48 mixture of BLG-A and BLG-B, and this might explain the lower values of pH_c for BLG-B compared with native BLG if (a) the binding of native BLG was dominated by the properties of BLG-A or (b) our measurement of affinity for native BLG reflected some "average" property of the two proteins. However, the second hypothesis would incorrectly suggest that pH_c for native BLG would be intermediate between values for A and B, but the first hypothesis incorrectly predicts that pH_c should always be lower for BLG-A. At the present time, the assumption that properties of "native BLG" can be treated simply as additive contributions from the A and B variants is uncertain. The difference in pH_ϕ, while subtle,

dx.doi.org/10.1021/bm101465y |*Biomacromolecules* XXXX, XXX, 000–000

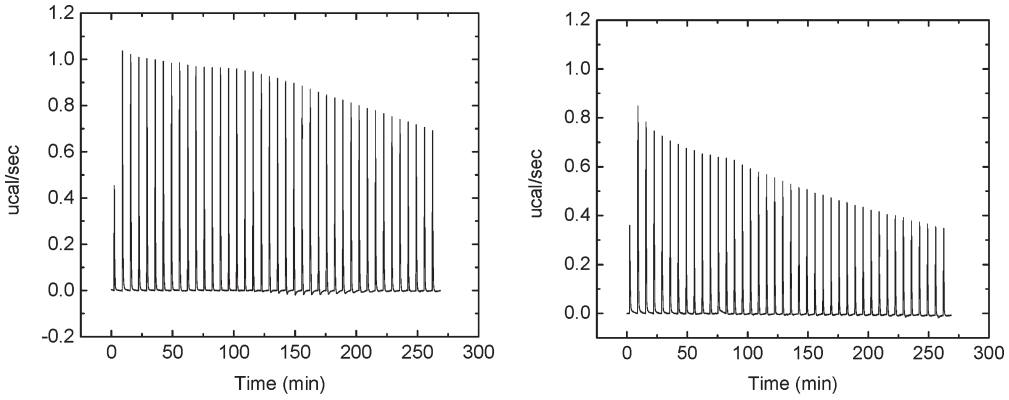

Figure 14. Isothermal titration calorimetry raw data of BLG-A-PDADMAC and BLG-B−PDADMAC. 1.2 mM (22.4 g/L for each) protein of each was used to titrate 0.00457 mM (1 g/L) PDADMAC. Buffer: 10 mM pH 7 phosphate, 140 mM NaCl. Each addition: 7 uL in 16.8 s, interval of injection: 400 s. 40 injections were made in the experiment. Heats of dilution were corrected by subtractions of blank titrations (PDADMAC−free).

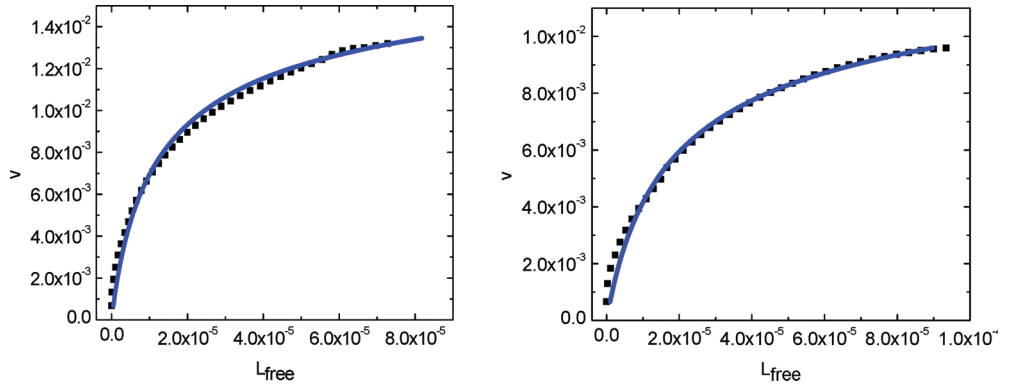

Figure 15. Binding isotherms of BLG-A−PDADMAC (left) and BLG-B−PDADMAC (right) transformed from Figure 14 at 25 °C dotted lines are experimental binding isotherms; solid lines are least-squares nonlinear fitting to eq 2.

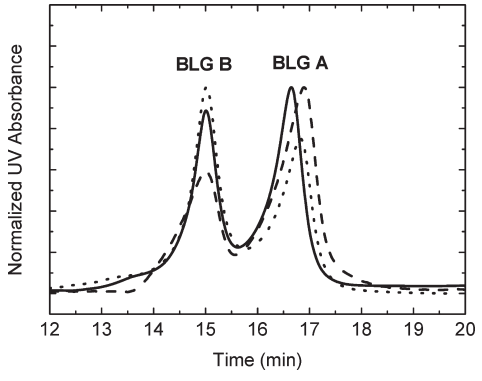

Figure 16. Ion exchange chromatography analysis of BLG-A and -B composition in different phases. Solid line: native BLG, dash line: coacervate, dotted line: supernatant. Featureless early elution chromatogram not shown.

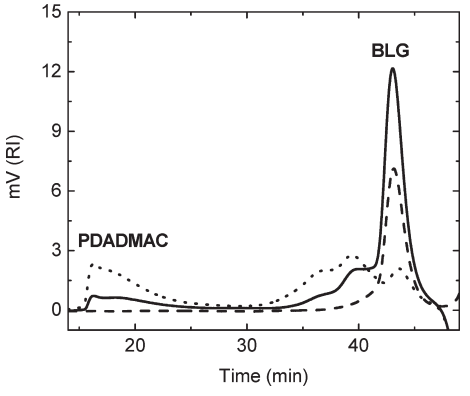

Figure 17. SEC analysis showing removal of PDADMAC by ultrafiltration. Before ultrafiltration: (a) coacervate, dissolved for SEC (solid line). After ultrafiltration: (b) ultrafiltrate (dashed line); (c) retentate (dotted line). Bimodality of the 35−41 min peak corresponds to BSA monomer/dimer.

does indicate conditions for selective coacervation with BLG-A as the target protein, to be presented later.

To ensure that the lower pH_c of BLG-A corresponds to a higher binding affinity, ITC was performed on BLG-A/PDADMAC and BLG-B/PDADMAC with the results shown in Figure 14. Endothermic reactions are observed for both BLG-A and -B at 150 mM salt compared with exothermic reactions observed for native BLG at 100 mM as described in Figure 7. Lin et al.[58] also found from ITC that the binding of BLG-A/-B to cationic Q-Sepharose gel was exothermic for $30 < I < 100$ mM and endothermic for $I = 200-300$ mM and ascribed this to

dx.doi.org/10.1021/bm101465y |*Biomacromolecules* XXXX, XXX, 000–000

Table 2. Polymer Removal and BLG Recovery Efficiency of 50 μL Coacervate[a]

	PDADMAC			BLG		
	concn (g/L)	volume (mL)	total PDADMAC (mg)	concn (g/L)	volume (mL)	total BLG (mg)
coacervate (before UF)	0.86 ± 0.05	0.60 ± 0.12	0.52 ± 0.21	3.17 ± 0.11	0.60 ± 0.13	1.90 ± 0.22
retentate	2.11 ± 0.06	0.30 ± 0.10	0.63 ± 0.33	0.27 ± 0.03	0.30 ± 0.12	0.08 ± 0.41
filtrate	0 ± 0	1.00 ± 0.4	0 ± 0	1.78 ± 0.07	1.00 ± 0.5	1.78 ± 0.54

[a] Apparent lack of mass balance for PDADMAC results from the large error in integrated areas at low retention times shown in Figure 17.

dominance of electrostatic interactions at low salt and hydrophobic interactions at high salt. Whereas an enhancement of hydrophobic interactions by a relatively small change in ionic strength appears unlikely, a more predominant favorable enthalpy from electrostatic interactions at low salt is reasonable, as pointed out recently by Sperber et al.[59] A global explanation of the variations in sign of ΔH for protein−polyelectrolyte interactions can be complicated by possible additional contributions from conformational changes, hydrophobic interactions, counterion binding/dissociation, and electrostatic interactions.[60,61] By fitting the binding isotherms transformed from the ITC thermograms, as described for BSA/BLG-PDADMAC (Figure 15), we obtained K_{obs} as 1500 ± 121 M^{-1} for BLG-A and 730 ± 16 M^{-1} for BLG-B. The larger K_{obs} of BLG-A is correlated with a larger heat absorbed upon binding to PDADMAC for BLG-A versus -B. Whereas this corresponds to a difference in binding energies of only about 2 kJ $mole^{-1}$ (<1 kT), it is a sufficient difference in binding affinity to lead to the shift in coacervation pH as shown in the phase diagram (Figure 13). Binding sites sizes n are obtained as 43 and 56 for BLG-A and -B, respectively, and the fact that they bracket n = 50 found for native BLG supports the accuracy of these values. The difference in n found for BLG-A and -B corresponds to a 30% increase in the maximum number of proteins bound per polymer chain n_{pr} (at pH 7, I = 150 mM), possibly a reflection of the higher binding affinity of BLG-A.

We tested the feasibility of selective coacervation of BLG-A and -B, as described above for BSA/BLG. Conditions of pH 6.3 and I = 100 mM were chosen to maximize ΔpH_ϕ based on the phase boundary shown in Figure 13. As a more practical demonstration of selective coacervation, we used native BLG (52% BLG-A) as the starting protein, increasing protein−polymer ratio (r) from 5 to 10 to reflect the lower concentration of the target protein. The two phases obtained after coacervation were analyzed by anion exchange chromatography (Figure 16), showing an increase in the BLG-A content of the coacervate to 66% BLG-A. This result for BLG-A/-B is notable considering the small ΔpH_ϕ, which could probably be enlarged by further optimization of I, pH and r.

3. Polyelectrolyte Removal. Finally, from a practical point of view, efficient removal of polyelectrolyte after phase separation with membrane ultrafiltration[62] was demonstrated in the BSA/BLG system. This technique, based on the larger molecular size of PDADMAC than proteins, is cheap, fast, and can be used in large scale compared with several other polyelectrolyte removal techniques including polyelectrolyte titration[63] and IEC.[64] To do this, the coacervate was dissolved and complexes were dissociated by lowering the pH to the uncomplexing condition pH ~3.5. Ultrafiltration with appropriate MW cutoff (100 kDa) was then used to remove polyelectrolyte from the target protein (BLG). After ultrafiltration, SEC analysis (Figure 17) was used to quantify PDADMAC and BLG in coacervate, retentate, and filtrate with the results shown in Table 2. The filtrate is found to contain >95% of the BLG and an essentially negligible amount of polyelectrolyte. These results suggest that ultrafiltration can efficiently remove the polyelectrolyte with little loss of protein, as long as the sizes of the PE and protein differ significantly.

CONCLUSIONS

Although the pIs of bovine BLG and bovine serum albumin (BSA) are very similar, the negative charge patch on BLG makes it possible to separate it from BSA by coacervation with the polycation poly(diallyldimethlammonium chloride) (PDADMAC). The crucial selection of pH and ionic strength conditions for selective coacervation was guided by phase boundaries for the two proteins, which present the ionic strength dependence of critical pH conditions corresponding to the onset of (1) complexation and (2) coacervation. Significant differences in the shapes of these plots for BSA and BLG arise from their different charge anisotropies, best visualized by DelPhi. Similar modeling for the two variants of BLG suggested that the two additional acidic amino acids in the dimer form of BLG-A enhance its negative charge patch, causing it to bind PDADMAC more strongly. This was confirmed qualitatively by a critical pH for PDADMAC complexation lower for BLG-A and quantitatively demonstrated by its larger binding constant measured by ITC. The prediction that this stronger binding of BLG-A would prevail in a mixture of the two isoforms was tested by PDADMAC coacervation of native BLG, and we obtained a two-fold increase in BLG-A content in a single step. Given the similarity of the two isoforms and the absence of any polymer-bound affinity ligand to provide specific protein recognition, the enhancement of BLG-A coacervation is remarkable. At a practical level, protein purification must be followed by removal of the polyelectrolyte, and the feasibility of ultrafiltration was demonstrated.

AUTHOR INFORMATION

Corresponding Author
*E-mail: dubin@chem.umass.edu.

ACKNOWLEDGMENT

Support from NSF (grant CBET-0966923) is acknowledged. We thank Dr. D. Julian McClements for access to the ITC instrument and Dr. Christophe Schmitt (Nestle, Lausanne, Switzerland) for the gift of BLG samples.

REFERENCES

(1) Shepard, S. R.; Boyd, G. A.; Schrimsher, J. L. *Bioseparation* **2001**, *10*, 51.

(2) Nfor, B. K.; Ahamed, T.; van Dedem, G. W. K.; van der Wielen, L. A. M.; van de Sandt, E. J. A. X.; Eppink, M. H. M.; Ottens, M. *J. Chem. Technol. Biotechnol.* **2008**, *83*, 124.
(3) Chen, J.; Nie, Z.-M.; Lü, Z.-B.; Zhu, C.-G.; Xu, C.-Z.; Jin, Y.-F.; Wu, X.-F.; Zhang, Y.-Z. *Appl. Biochem. Biotechnol.* **2007**, *141*, 149.
(4) Kamarck, M. E. *Nat. Biotechnol.* **2006**, *24*, 503.
(5) Lico, C.; Chen, Q.; Santi, L. *J. Cell Physiol.* **2008**, *216*, 366.
(6) Dove, A. *Nat. Biotechnol.* **2002**, *20*, 777.
(7) Kelley, B. *Biotechnol. Prog.* **2007**, *23*, 995.
(8) Meyer, V. R. *Practical High-Performance Liquid Chromatography*; Wiley: Chichester, U.K.,2010.
(9) Ghosh, R. *J. Chromatogr., A* **2002**, *952*, 13.
(10) Fong, B. A.; Wu, W.-Y.; Wood, D. W. *Protein Expression Purif.* **2009**, *66*, 198.
(11) Simpson, R. J. *Purifying Proteins for Proteomics*; Cold Spring Harb Protoc, Cold Spring Harbor Laboratory Press: Cold Spring Harbor, NY, 2006; Appendix 3.
(12) Izumrudov, V.; Galaev, I.; Mattiasson, B. *Bioseparation.* **1998**, *7*, 207.
(13) Boeris, V.; Spelzini, D.; Salgado, J. P.; Picó, G.; Romanini, D.; Farruggia, B. *Biochim. Biophys. Acta* **2008**, *1780*, 1032.
(14) Zhang, C.; Lillie, R.; Cotter, J.; Vaughan, D. *J. Chromatogr., A* **2005**, *1069*, 107.
(15) Peram, T.; McDonald, P.; Carter-Franklin, J.; Fahrner, R. *Biotechnol. Prog.* **2010**, *26*, 1322.
(16) Scopes, K. R. *Protein Purification: Principles and Practice*, 3rd ed.; Springer-Verlag: New York, 1994; p 71.
(17) Boeris, V.; Romanini, D.; Farruggia, B.; Picó, G. *Process Biochem.* **2009**, *44*, 588.
(18) Braia, M.; Porfiri, M. C.; Farruggia, B.; Picó, G.; Romanini, D. *J. Chromatogr., B* **2008**, *873*, 139.
(19) Holler, C.; Vaughan, D.; Zhang, C. *J. Chromatogr., A* **2007**, *1142*, 98.
(20) Holler, C.; Zhang, C. *Biotechnol. Bioeng.* **2008**, *99*, 902.
(21) Dubin, P. L.; Gao, J.; Mattison, K. *Sep. Purif. Methods* **1994**, *23*, 1.
(22) Kaibara, K.; Okazaki, T.; Bohidar, H. B.; Dubin, P. L. *Biomacromolecules* **2000**, *1*, 100.
(23) Xia, J.; Mattison, K.; Romano, V.; Dubin, P. L.; Muhoberac, B. B. *Biopolymers* **1997**, *41*, 359.
(24) Kayitmazer, A. B.; Shaw, D.; Dubin, P. L. *Macromolecules* **2005**, *38*, 5198.
(25) Mattison, K. W.; Dubin, P. L.; Brittain, I. J. *J. Phys. Chem. B* **1998**, *102*, 3830.
(26) Hattori, T.; Hallberg, R.; Dubin, P. L. *Langmuir*. **2000**, *16*, 9738.
(27) Mattison, K. W.; Brittain, I. J.; Dubin, P. L. *Biotechnol. Prog.* **1995**, *11*, 632.
(28) Xia, J.; Dubin, P. L.; Morishima, Y.; Sato, T.; Muhoberac, B. B. *Biopolymers* **1995**, *35*, 411.
(29) Kayitmazer, A. B.; Bohidar, H. B.; Mattison, K. W.; Bose, A.; Sarkar, J.; Hashidzume, A.; Russo, P. S.; Jaeger, W.; Dubin, P. L. *Soft Matter* **2007**, *3*, 1064.
(30) Seyrek, E.; Dubin, P. L.; Tribet, C.; Gamble, E. A. *Biomacromolecules* **2003**, *4*, 273.
(31) Turgeon, S. L.; Schmitt, C.; Sanchez, C. *Curr. Opin. Colloid Interface Sci.* **2007**, *12*, 166.
(32) Bohidar, H.; Dubin, P. L.; Majhi, P. R.; Tribet, C.; Jaeger, W. *Biomacromolecules* **2005**, *6*, 1573.
(33) Kayitmazer, A. B.; Strand, S. P.; Tribet, C.; Jaeger, W.; Dubin, P. L. *Biomacromolecules* **2007**, *8*, 3568.
(34) Lee, W.-C.; Lee, K. H. *Anal. Biochem.* **2004**, *324*, 1.
(35) Hedhammar, M.; Gräslund, T.; Hober, S. *Chem. Eng. Technol.* **2005**, *28*, 1315.
(36) Yamamoto, S. *Chem. Eng. Technol.* **2005**, *28*, 1387.
(37) Yamamoto, S.; Ishihara, T. *J. Chromatogr., A* **1999**, *852*, 31.
(38) Ye, X.; Yoshida, S.; Ng, T. B. *Int. J. Biochem. Cell Biol.* **2000**, *32*, 1143.
(39) Mollerup, J. M.; Hansen, T. B.; Kidal, S.; Sejergaard, L.; Staby, A. *Fluid Phase. Equilib.* **2007**, *261*, 133.
(40) Grymonpré, K. R.; Staggemeier, B. A.; Dubin, P. L.; Mattison, K. W. *Biomacromolecules* **2001**, *2*, 422.
(41) Seyrek, E.; Dubin, P. L.; Henriksen, J. *Biopolymers.* **2007**, *86*, 249.
(42) Antonov, M.; Mazzawi, M.; Dubin, P. L. *Biomacromolecules* **2009**, *11*, 51.
(43) Wang, Y.; Gao, J. Y.; Dubin, P. L. *Biotechnol. Prog.* **1996**, *12*, 356.
(44) Dautzenberg, H.; Görnitz, E.; Jaeger, W. *Macromol. Chem. Phys.* **1998**, *199*, 1561.
(45) Tomme, P.; Creagh, A. L.; Kilburn, D. G.; Haynes, C. A. *Biochemistry* **1996**, *35*, 13885.
(46) Girard, M.; Turgeon, S. L.; Gauthier, S. F. *J. Agric. Food Chem.* **2003**, *51*, 4450.
(47) McGhee, J. D.; von Hippel, P. H. *J. Mol. Biol.* **1974**, *86*, 469.
(48) Nicholls, A.; Honig, B. *J. Comput. Chem.* **1991**, *12*, 435 .
(49) Tanford, C.; Kirkwood, J. G. *J. Am. Chem. Soc.* **1957**, *79*, 5333.
(50) Tanford, C.; Swanson, S. A.; Shore, W. S. *J. Am. Chem. Soc.* **1955**, *77*, 6414.
(51) Nozaki, Y.; Bunville, L. G.; Tanford, C. *J. Am. Chem. Soc.* **1959**, *81*, 5523.
(52) Hattori, T.; Kimura, K.; Seyrek, E.; Dubin, P. L. *Anal. Biochem.* **2001**, *295*, 158.
(53) Hattori, T.; Bat-Aldar, S.; Kato, R.; Bohidar, H. B.; Dubin, P. L. *Anal. Biochem.* **2005**, *342*, 229.
(54) Dong, A.; Matsuura, J.; Allison, S. D.; Chrisman, E.; Manning, M. C.; Carpenter, J. F. *Biochemistry* **1996**, *35*, 1450.
(55) Huang, X. L.; Catignani, G. L.; Swaisgood, H. E. *J. Agric. Food Chem.* **1994**, *42*, 1276.
(56) Majhi, P. R.; Ganta, R. R.; Vanam, R. P.; Seyrek, E.; Giger, K.; Dubin, P. L. *Langmuir* **2006**, *22*, 9150.
(57) Vanam, R. P. Thesis, *Purdue Univeristy*, 2004.
(58) Lin, F.-Y.; Chen, C.-S.; Chen, W.-Y.; Yamamoto, S. *J. Chromatogr., A* **2001**, *912*, 281.
(59) Sperber, B. L. H. M.; Cohen Stuart, M. A.; Schols, H. A.; Voragen, A. G. J.; Norde, W. *Biomacromolecules* **2010**, *11*, 3578.
(60) Harnsilawat, T.; Pongsawatmanit, R.; McClements, D. J. *Food Hydrocolloids* **2006**, *20*, 577.
(61) Aberkane, L. l.; Jasniewski, J.; Gaiani, C.; Scher, J. l.; Sanchez, C. *Langmuir* **2010**, *26*, 12523.
(62) Kasperchik, V. P.; Yaskevich, A. L.; Bil'dyukevich, A. V. *Colloid J.* **2003**, *65*, 579.
(63) Parazak, D. P.; Burkhardt, C. W.; McCarthy, K. J. *Anal. Chem.* **1987**, *59*, 1444.
(64) McDonald, P.; Victa, C.; Carter-Franklin, J. N.; Fahrner, R. *Biotechnol. Bioeng.* **2009**, *102*, 1141.